DAMAGE PREDICTION IN WOVEN CFRP LAMINATE PLATES CAUSED BY LOW VELOCITY IMPACT

ROMARIZ, L.A., la.romariz@gmail.com
ALVES, M., maralves@usp.br
Group of Solid Mechanics and Structural Impact (GMSIE), Dep. of Mechatronics and Mechanical System Engineering,
Polytechnical School of University of Sao Paulo,
Av. Prof. Mello de Moraes 2231, São Paulo, SP, Brazil, 05508-030

Abstract. *This article presents the development of a numerical simulation methodology that estimates damage in laminate plate caused by low velocity impact. Experimental tests were performed on laminate plates reinforced with woven carbon fibers and epoxi resine. Three thickness plates were evaluated. The impact loads, transversal and punctual were achieved with a drop-test machine, in therange between 5J and 94J, and velocities lower than 6m/s. Numerical simulations of the tests were performed with a commercial explicit FEM code. Two lamina failure criteria were evaluated: the maximum stress and a modification of the Hashin failure criterion. The numerical contact loads between the plate and impactor were well represented. The numerical damaged areas and lengths were similar or greater than the experimental results.*

Keywords: *Composite; Damage strength; Degradation criteria; Failure criteria; Impact load*

1. INTRODUCTION

The Carbon Fiber Reinforced Polymer (CFRP) laminate has an excellent combination of stiffness, strength and low weight which are very good features for the development of lightweight structures. However, low velocity impact damage in laminate composite has been recognized as a debilitating threat in aerospace structure projects and other high performance vehicles (Davies and Zhang, 1994).

Carbon fiber is elastic and brittle, and so it is the epoxy matrix. According to Richardson and Wisheart (1996), these laminates can only absorb energy in elastic deformation and through damage mechanism, not via plastic deformation. These composites material can fail in a wide variety of modes and contain barely visible impact damage (BVID) which nevertheless severely reduces the structural integrity of component.

Many works and researches have been developed aiming at studying the behavior of composites under low velocity impact. One of them is the damage resistance analysis. According to Cairns and Lagace (1992), the damage resistance analysis defines the loads a structure is able to withstand without failure. If material failure happens, this analysis shall determine the amount and the type of damage. To accurately predict damage in laminate plates caused by impact loads is a challenge, due to anisotropy, heterogeneity, and complex failure models (Feraboli and Kedward, 2004).

Hinton and Soden (1998) and Icardi (2007) found that the failure criteria for composite laminate materials are not accurate for the various cases of loads, boundary conditions, fiber materials and directions, matrix materials, lay-ups and thicknesses. Davies and Zhang (1994) concluded that the use of simple plate finite element models to predict force histories works well, if in-plane degradation is considered in the numerical analysis. According to Mathews (1994), there is not a universal degradation criterion agreement yet.

In this paper, some degradation criteria were investigated as well as two in-plane laminate failure criteria were evaluated in this article: the maximum stress and a proposed modification of the Hashin failure criterion. Experimental tests are also presented and support the findings reported here.

2. LAMINA FAILURE CRITERIA

The lamina strength stresses X_t, X_c, Y_t, Y_c and S were obtained with standard one-dimensional tensile tests. X is the strength stress in 1 direction and Y on the 2 direction. The subscript t and c are respectively tension and compression. S is the shear strength in the laminate plane 12. The interlaminar shear strength in the laminate plane 31 is considered equal to the one in the laminate plane 23, and it is called S_2.

Mendonça (2005) mentions that the maximum stress failure criterion was proposed by Jenkins in 1920. This theory is very popular and states that the material fails when one of the principal stresses reaches the strength stress in its load direction. For the lamina, there are five different equations, without interaction among the strength stresses:

$$\frac{\sigma_1}{X_T}=1\,,\ \frac{|\sigma_1|}{X_C}=1\,,\ \frac{\sigma_2}{Y_T}=1\,,\ \frac{|\sigma_2|}{Y_C}=1\,,\ \frac{|\tau_{12}|}{S}=1 \tag{1}$$

The original Hashin failure criterion was developed for unidirectional fibers (Hashin, 1980) with failure equations for each material failure mode which consider the physical dependence among the stresses.

Here, we modify the Hashin criterion were by adding the shear failure mode due the shear stress 12, and the original tension and compression fiber failure equations were applied to the lamina direction 1 and 2.

The equation for failure mode caused by tension on lamina direction 1 ($\sigma_1 > 0$) is

$$\left(\frac{\sigma_1}{X_T}\right)^2 + \left(\frac{\tau_{12}}{S}\right)^2 = 1 \tag{2}$$

The equation for failure mode caused by compression on lamina direction 1 ($\sigma_1 < 0$) is

$$-\frac{\sigma_1}{X_C} = 1 \tag{3}$$

The failure mode due to tension on lamina direction 2 ($\sigma_2 > 0$) is

$$\left(\frac{\sigma_2}{Y_T}\right)^2 + \left(\frac{\tau_{12}}{S}\right)^2 = 1 \tag{4}$$

While compression on lamina direction 2 ($\sigma_2 < 0$) failure is given by

$$-\frac{\sigma_2}{X_C} = 1 \tag{5}$$

The equation for failure mode caused by Shear on lamina plane 12 is:

$$\frac{|\tau_{12}|}{S} = 1 \tag{6}$$

In the present numerical analysis, Eq. (7) for the failure criterion caused by compression on lamina direction 2 was adopted. Equation (7) is the original Hashin failure equation for matrix under compression. However, if the equation (5) were used, the numerical results would be very similar. This is due to the great influence of the Eq. (6) when applied using the present material data.

$$\left(\frac{\sigma_2}{2S_2}\right)^2 + \left[\left(\frac{Y_c}{2S_2}\right)^2 - 1\right]\frac{\sigma_2}{Y_c} + \left(\frac{\tau_{12}}{S}\right)^2 = 1 \tag{7}$$

Figure 1 presents the various failure curves. Due the bidirectional fiber orientations, the woven fabric lamina should have similar failure criteria in directions 1 and 2. Comparing with the "Modified Hashin" and the maximum stress failure curves, the differences are greater when σ_1 or σ_2 are positives.

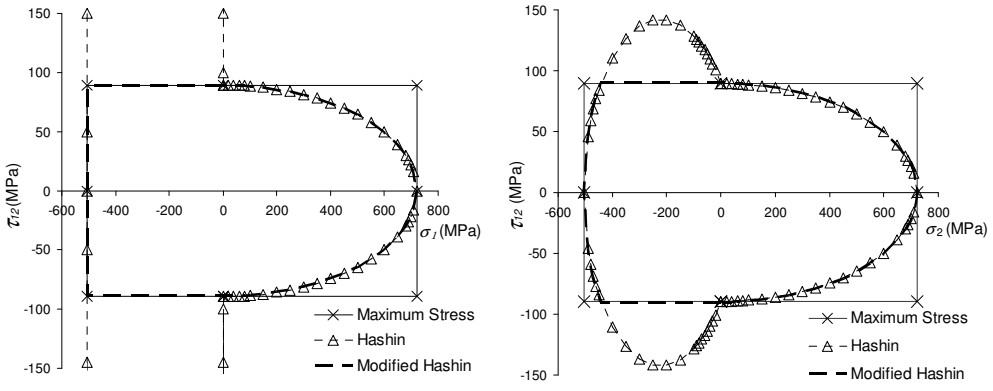

(a) (b)

Figure 1. Failure criteria curves: (a) σ_1 x τ_{12} (b) σ_2 x τ_{12}.

3. LAMINA DEGRADATION CRITERIA

Four lamina degradation criteria *D01*, *D02*, *D03* and *D04* are proposed and evaluated in this article.

Table 1 lists the material property degradations for each failure mode valid for the D01 degradation criterion. The elastic modulus is degraded to zero in the same failure mode stress direction.

Table 1. Material properties degraded with *D01* criterion.

Failure mode	Degraded properties			
Tension on the direction 1	$E_1=0$		$\nu_{12}=0$	$G_{12}=0$
Compression on the direction 1	$E_1=0$		$\nu_{12}=0$	
Tension on the direction 2		$E_2=0$	$\nu_{12}=0$	$G_{12}=0$
Compression on the direction 2		$E_2=0$	$\nu_{12}=0$	
Shear in-plane 12				$G_{12}=0$

Comparing to the *D01* degradation criterion, the *D02* reduces to zero the elastic modulus and the Poisson coefficient when shear in-plane 12 failure happens. Table 2 presents this failure model and the degraded properties.

Table 2. Material properties degraded with *D02* criterion.

Failure model	Degraded properties		
Shear in-plane 12	$E_2=0$	$\nu_{12}=0$	$G_{12}=0$

Comparing to the *D01* degradation criterion, the *D03* reduces to zero the elastic modulus in directions 1 and 2 when failure by tension in direction 1 happens, Table 3.

Table 3. Material properties degraded with *D03* criterion.

Failure model	Degraded properties			
Tension on the direction 1	$E_1=0$	$E_2=0$	$\nu_{12}=0$	$G_{12}=0$

Lastly, comparing to the *D01* degradation criterion, the *D04* reduces to zero the elastic modulus in directions 1 and 2 when failure by tension or compression in direction 1 happens, Table 4.

Table 4. Material properties degraded with *D04* criterion.

Failure model	Degraded properties			
Tension on the direction 1	$E_1=0$	$E_2=0$	$\nu_{12}=0$	$G_{12}=0$
Compression on the direction 1	$E_1=0$	$E_2=0$	$\nu_{12}=0$	

4. EXPERIMENAL TEST

Figure 2 (a) presents the rig for the low velocity impact tests. It is a drop test based on the ASTM D5628-96 (2001), but the plate dimension and instrumentations were specifically defined for this research.

The steel impactor in Fig. 2(b) has a total mass of 11,01 kg.

Figure 3 presents the test specimen and the rigid supports geometry. Laminate plates $[0,90]_{10}$, $[0,90]_{20}$ e $[0,90]_{30}$ were tested with the plate thicknesses being 2.1mm, 4.2mm e 6.3mm.

One accelerometer measured the impact velocity and the impact energy, while a second one measured the impact force along time. A fast Fourier transform low pass filter at 2500 Hz was applied on the acceleration results to remove the impactor free vibration.

After impact, the damage area on the plate was inspected with C-scan. The inspections on the two plate surfaces were performed to find any delamination between internal laminas. The delamination area was mapped with discrete squares with 5mm length., Fig. 4. The damage area A_d is calculated as the sum of these squares. h_m is the greatest damage linear length.

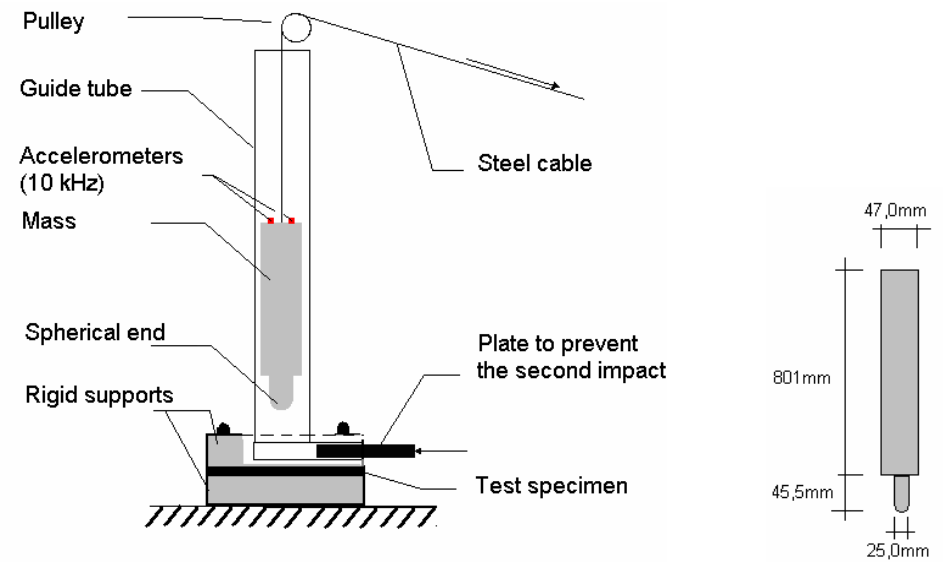

Figure 2. Drop test: (a) Rig (b) Impactor.

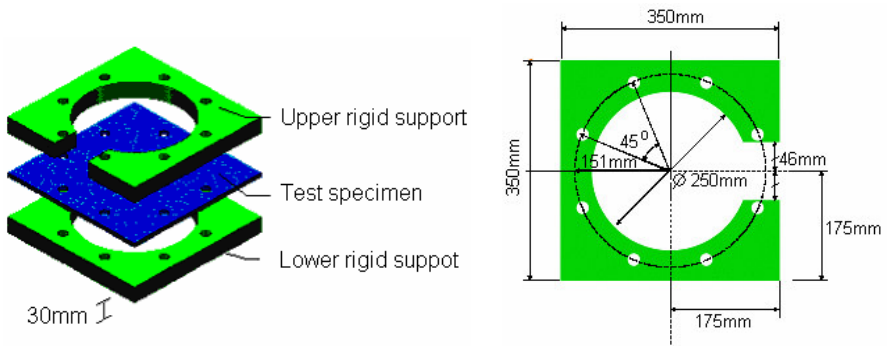

Figure 3. Test specimen and rigid support geometry.

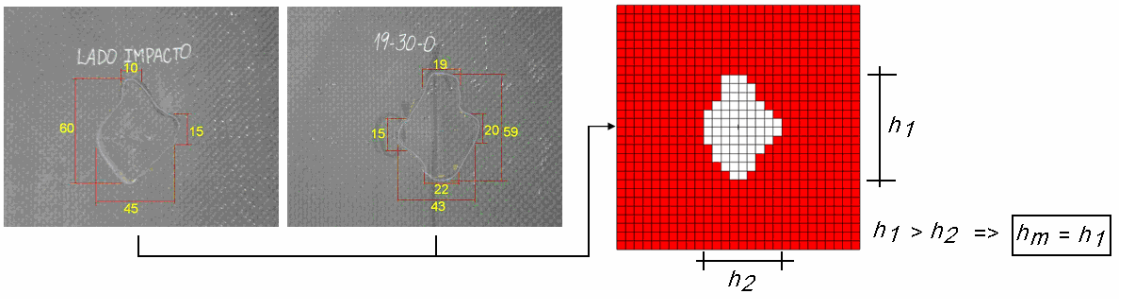

Figure 4. Approach to map the experimental delamination area on the laminate plate.

5. NUMERICAL SIMULATIONS

The numerical simulation was performed with the commercial finite element explicit code MSC/Dytran 2007. This code has laminate plate elements as well as the maximum stress failure criterion. The "Modified Hashin" criterion was performed in this code with a combination of Hashin and the maximum stress failure criteria. The four degradation criteria (*D01, D02, D03* and *D04*) were configured with input commands in the code. The properties were degraded linearly in 100 time steps.

Plate elements based on the Middlen-Reissner cinematic theory were used to model the plates, Fig. 5.

In the laminate plate, enforced zero translation displacements were applied on the nodes at bolts locations, Fig. 5(a). The mesh size is 5mm length. Rigid plate elements modeled the upper and the lower supports, Fig 5(b). Their nodes were fixed. The contacts between the laminate plate and the supports were also modeled. There are not gaps and friction forces.

The impactor end mesh was more detailed than the laminate plate mesh, Fig. 5(c). It was represented with rigid shell elements. The contact between the plate and the impactor end was modeled too. Bar elements with 2 axial degrees of freedoms modeled the impactor body.

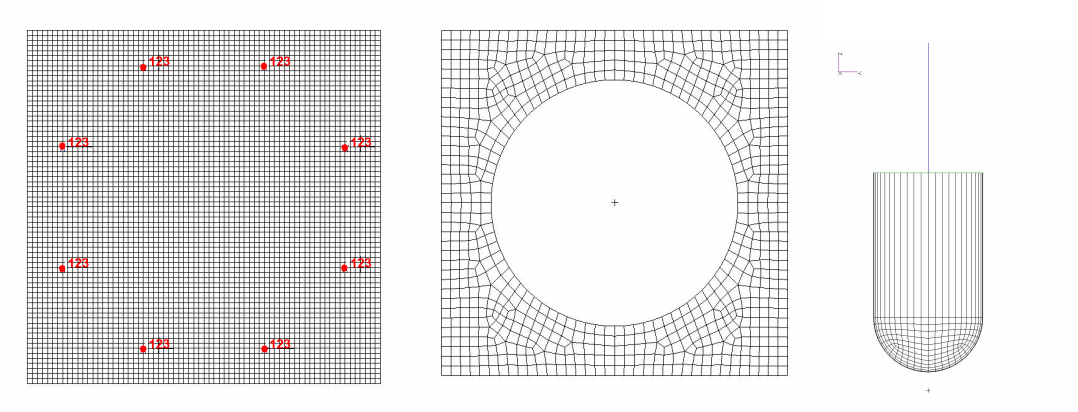

(a) (b) (c)

Figure 5. Shell element meshes. (a) Laminate plate and pinned nodes at bolt positions; (b) Rigid supports; (c) Lateral view of the impactor.

Table 4 presents the laminate mechanical properties based on Romariz (2008), being assumed that $E_1 = E_2$, $G_{12} = G_{23} = G_{31}$, $X_t = Y_c$, $X_c = Y_c$, $S = S_2$.

Table 4. Material properties.

Symbol	Value	Property
E_1	62.50 GPa	Elastic modulus in the lamina direction 1.
E_2	62.50 GPa	Elastic modulus in the lamina direction 2.
G_{12}	4.54 GPa	Shear modulus in the lamina plane 12.
G_{23}	4.54 GPa	Shear modulus in the lamina plane 23.
G_{31}	4.54 GPa	Shear modulus in the lamina plane 31.
ν_{12}	0.05	Poisson coefficient 12.
X_t	721.6 MPa	Tensile strength in the lamina direction 1.
X_c	505.4 MPa	Compressive strength in the lamina direction 1.
Y_t	721.6 MPa	Tensile strength in the lamina direction 2.
Y_c	505.4 MPa	Compressive strength in the lamina direction 2.
S	89.4 MPa	In-plane shear strength.
S_2	89.4 MPa	Interlaminar shear strength.

6. RESULTS AND ANALYSIS

6.1. ACTING FORCES ON THE IMPACTOR

The impactor energy after impact (E_r), the time period of impact (T_{imp}), the maximum force (F_{max}) and the damage threshold force (F_{th}) are parameters used to compare the numerical models and the experimental results.

Based in Hinton (2002), the difference between the numerical and the experimental results are classified with grades. According to the absolute percentage difference between the numerical model result and the one that was the closest to the experimental result, a grade was given to each parameter. Table 5 presents these grades as a function of the result ranges for each parameter.

The numerical simulation grade is the sum of the parameter grades. Table 6 presents the numerical simulation grades obtained with different model simulations, impact energies and plate thicknesses.

Table 5. Grades according to the absolute percentage difference between the numerical model result and the one that was the closest to the experimental result for each parameter.

Parameter	absolute percentage difference		
F_{th}	0% a 1%	1% a 10%	>10%
F_{max}	0% a 10%	10% a 20%	>20%
T_{imp}	0% a 5%	5% a 10%	>10%
E_r	0% a 10%	10% a 20%	>20%
Grades	**2**	**1**	**0**

Table 6. Numerical simulation grades obtained with different models, impact energies and plate thicknesses.

Plate	E_i (J)	**MS D01**	**MS D02**	**MS D03**	**MS D04**	**MH D01**	**MH D02**	**MH D03**	**MH D04**
$[0,90]_{10}$	11.6	4	3	4	4	6	6	7	2
	13.7	6	5	5	5	4	6	7	2
	22.7	4	6	5	4	6	7	7	2
	32.4	6	6	6	6	6	6	2	2
$[0,90]_{20}$	30.6	7	8	8	8	7	7	8	8
	42.5	7	7	8	7	7	8	7	7
	55.8	7	6	6	6	7	7	7	6
	65.1	6	6	6	6	6	6	6	6
$[0,90]_{30}$	44.5	8	7	8	8	7	7	8	7
	54.6	7	7	7	8	7	8	7	7
	63.3	8	8	8	8	8	8	8	8
	94.3	6	6	6	6	6	6	6	6

MS is Maximum Stress failure criterion and MH is "Modified Hashin" failure criterion.

Accordingly, if a numerical model has a grade equal or grater than 6, it means that the force curve is similar to the best one obtained from the numerical model. Table 7 presents the numerical models with grades ≥ 6, considering different impact energy ranges for each plate thickness.

Table 7. Numerical models with the best force results.

Plate	E_i (J)	Models
$[0,90]_{10}$	11.6J to 22.7J	Modified Hashin D02
		Modified Hashin D03
	11.6J to 32.4J	Modified Hashin. D02
$[0,90]_{20}$	30.6J to 55.8J	Modified Hashin. D01
		Modified Hashin D02
		Modified Hashin D03
		Maximum Stress D01
	30.6J to 65.1J	Modified Hashin D01
		Modified Hashin D02
		Maximum Stress D01
$[0,90]_{30}$	44.5J to 63.3J	All models
	44.5J to 94.3J	All models, except Maximum Stress D02

It is clear from Table 7 that "Modified Hashin D02" model performs better for all impact energies and plate thicknesses.

Figure 6 to 8 compare the numerical and experimental impactor forces for the cases $[0,90]_{10}$, $[0,90]_{20}$ and $[0,90]_{30}$ respectively. The forces were normalized by the experimental threshold force (F_{th}). The numerical impactor forces are in good agreement with the experimental results.

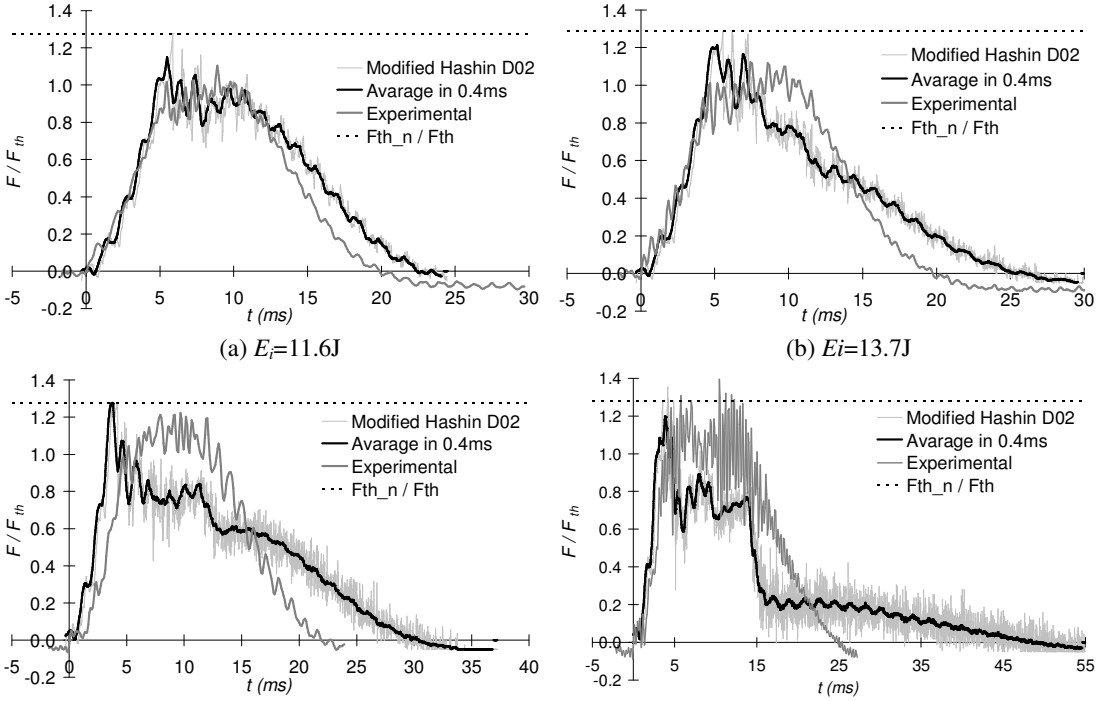

(a) E_i=11.6J (b) Ei=13.7J

(c) E_i=22.7J (d) Ei=32.4J

Figure 6. Comparisons between numerical and experimental impactor forces, plate $[0,90]_{10}$.

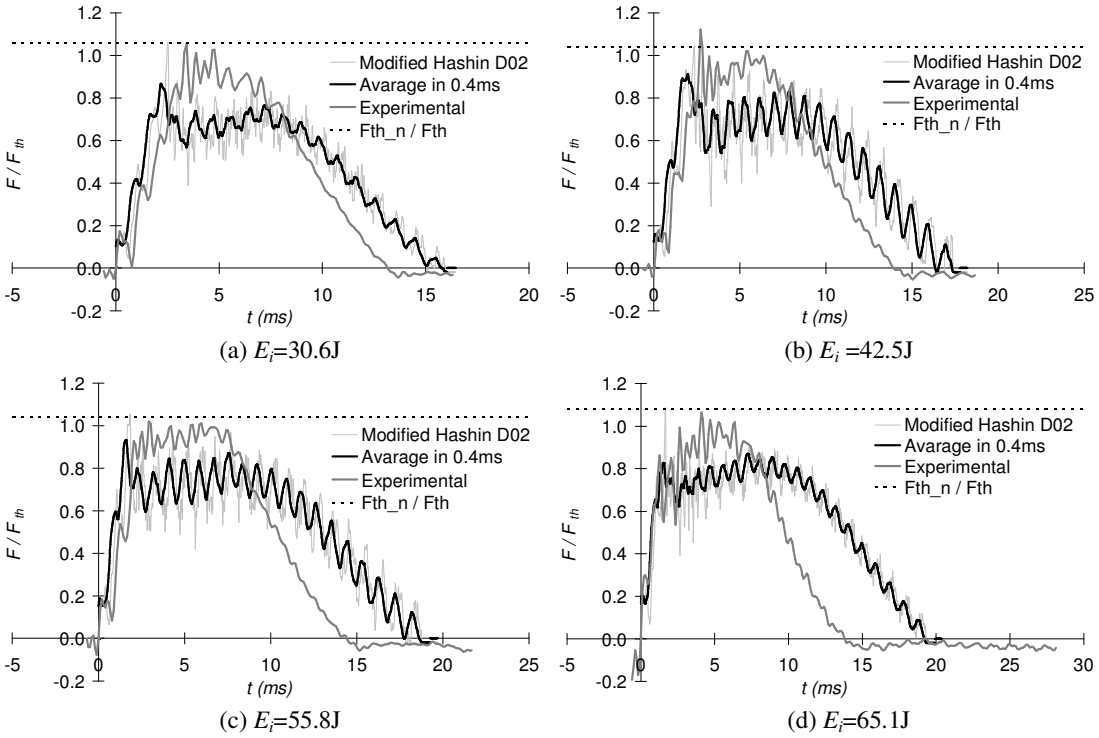

(a) E_i=30.6J (b) E_i =42.5J

(c) E_i=55.8J (d) E_i=65.1J

Figure 7. Comparisons between numerical and experimental impactor forces, plate $[0,90]_{20}$.

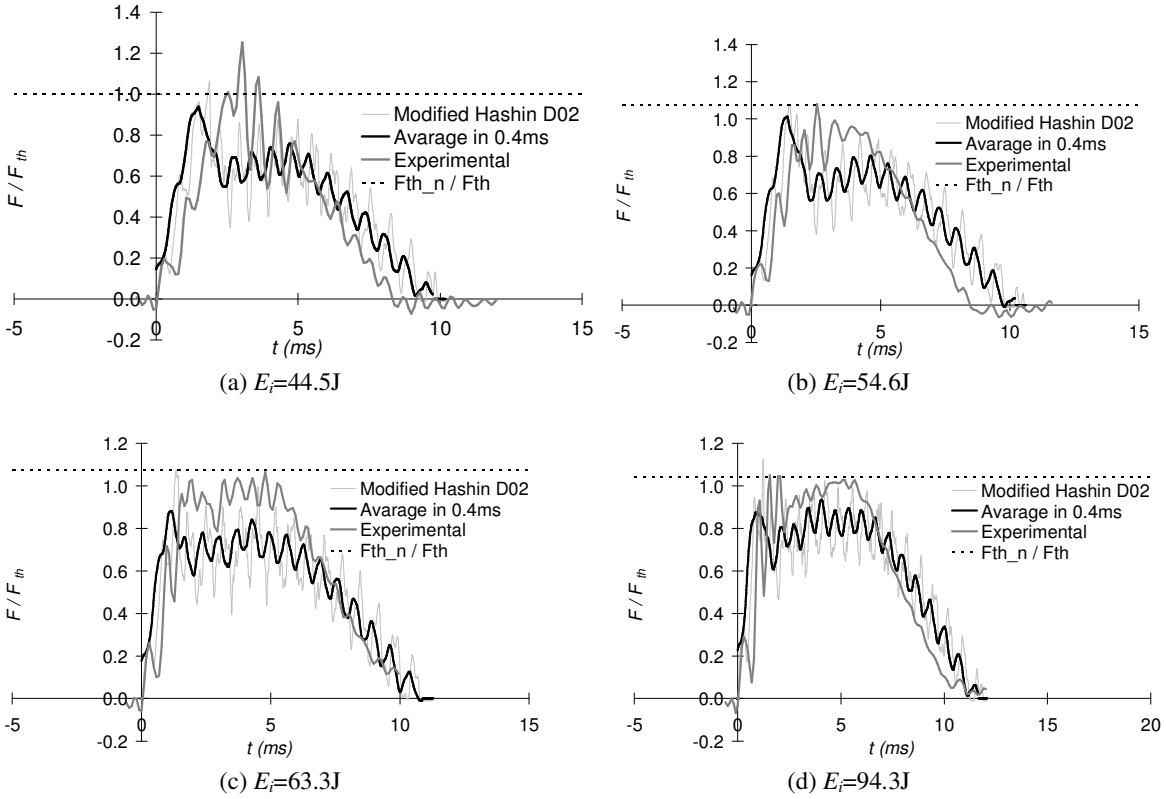

(a) E_i=44.5J (b) E_i=54.6J

(c) E_i=63.3J (d) E_i=94.3J

Figure 8. Comparisons between numerical and experimental impactor forces, plate $[0,90]_{30}$.

6.2. DAMAGE ON PLATES

Figure 9 presents the experimental trend curves of the damage area (A_d) versus the impact energy (E_i). A linear dependency was also noticed by Abrate (1998). The damage area was normalized by A_{d_ref}., the damage area in a plate $[0,90]_{30}$ impacted with an energy of E_i = 44J. This area is about 550 mm^2.

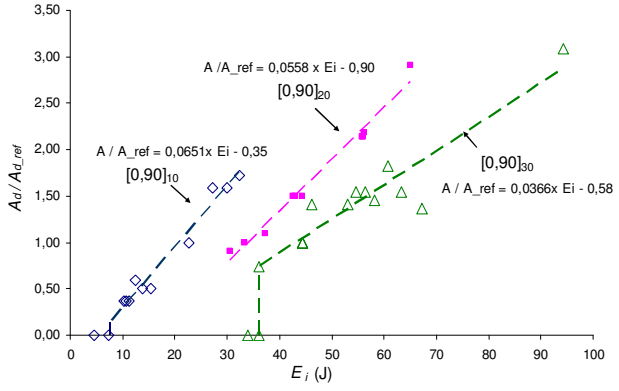

Figure 9. Experimental damage area versus the impact energy.

Table 8 presents the percent difference between the numerical and the experimental damaged area. The numerical damage areas are greater than the experimental ones.

Checking the experimental damage shapes after impact, they are well represented with a square with diagonal h_m. Equation (8) gives the area of a square with diagonal (C_a . h_m). Based on the experimental damage areas and the numerical h_m results, a correction factor (C_a) was calculated for each laminate thickness, Tab. 9.

$$A_{d\_corrected} = \frac{(C_A h_m)^2}{2} \tag{8}$$

Table 8. Difference of the numerical damage area to the experimental results.

Plate	E_i (J)	MS D01	MS D02	MS D03	MS D04	MH D01	MH D02	MH D03	MH D04
$[0,90]_{10}$	11,6	(1)	(1)	(1)	(1)	(1)	204%	260%	(1)
	13,7	(1)	(1)	(1)	(1)	(1)	193%	193%	(1)
	22,7	(1)	(1)	(1)	(1)	(1)	143%	171%	(1)
	32,4	(1)	(1)	(1)	(1)	(1)	138%	(1)	(1)
$[0,90]_{20}$	30,6	127%	(1)	(1)	(1)	121%	104%	87%	(1)
	42,5	79%	(1)	(1)	(1)	82%	70%	70%	(1)
	55,8	48%	(1)	(1)	(1)	44%	40%	42%	(1)
	65,1	53%	(1)	(1)	(1)	45%	27%	(1)	(1)
$[0,90]_{30}$	44,5	48%	43%	39%	26%	35%	43%	48%	56%
	54,6	41%	48%	28%	41%	32%	45%	54%	32%
	63,3	28%	23%	39%	18%	31%	39%	28%	28%
	94,3	1%	(1)	-5%	8%	17%	17%	17%	8%

Notes: (1) Numerical model was not selected on Tab. 7.

Table 9. Correction fator C_a.

Plate	$[0,90]_{10}$	$[0,90]_{20}$	$[0,90]_{30}$
C_a	0.75	0.50	0.60

Figure 10 compares the A_d calculated with this correction factor C_a and the experimental test results. The numerical model uses the "Modified Hashin" failure criteria and the damage criteria "*D02*".

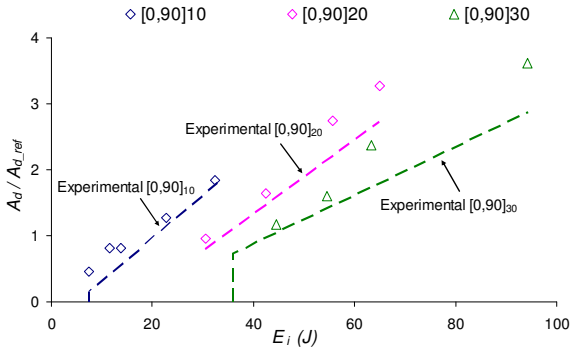

Figure 10. Comparison between the experimental A_d and numerical A_d with correction factor C_a.

Based on the Fig. 10, this correction procedure on the numeric results will give better damage areas. This methodology to predict damage in woven CFRP laminate plates can be performed if the impact energy is in the range tested on this work and the impactor velocity is less than 6 m/s. Extrapolation is not recommended because the material failure mode may change.

7. CONCLUSIONS

The dynamic numeric simulation using laminate plate elements, applying the numeric correction methodology based on the experimental tests performed in this work gives a good prediction of the low impact damage on laminate plate.

Based on the analysis, the numerical model with 'Modified Hashin" failure criterion and "D02" degradation criterion is the numerical model that gives the best results considering all the thicknesses and impact energies tested.

Comparing with the experimental results, the impactor actuating forces were well represented numerically. However, the numerical damage areas using the 'Modified Hashin D02" model were always greater than the

experimental ones. In order to have a better damage area prediction, it was proposed a damage area correction on the numerical models results.

This numerical methodology can yield good predictions of damage area caused by impact on structure parts. But it can be applied with some limitations: the structural material shall be made of epoxy resin reinforced with carbon fiber woven, the plate thickness shall be between 10 and 30 plies, the lay up shall be in directions [0,90] and the impact energy shall be in the range tested in this work with impact velocities less than 6 m/s.

Future researches can use the same experimental and numerical methodology to select good failure criteria and degradation criteria to predict impact damage in other laminate materials (unidirectional fibers, aramid fibers and glass fibers), other lay-ups and other levels of impact energies.

8. REFERENCES

Abrate, S., 1998, "Impact on composite structures", Ed. Cambridge University, Cambridge.

ASTM D5628-96**,** 2001, "Standart test method for impact resistance of flat, rigid plastic specimens by means of falling dart (Tup por falling mass)", American Society for Testing and Materials , West Conshohoken, PA.

Cairns, D.S. and Lagace, P.A., 1992, "A Consistent Engineering Methodology for the Treatment of Impact in Composite Materials*",* Journal of Reinforced Plastics and Composites; Vol.11, n. 4, pp. 395-412.

Davies, G.A.O. and Zhang, X., 1995, "Impact damage prediction in carbon composite structures", International Journal of Impact Engineering, Vol. 16, n. 1, pp. 149-170.

Feraboli, P. and Kedward, K.T., 2004, "Enhaced evaluation of the low-velocity impact response of composite plates", AIAA Journal, Vol.42, n. 10, pp. 2143-2152.

Hashin, Z., 1980, "Failure criteria for unidiretional fiber composites", Journal of Applied Mechanics, Vol.47, pp. 329-334.

Hinton, M.J.; Soden, P.D., 1998, "Predicting failure in composite laminates: the background to the exercise", Composites Science and Technology, Vol.58, n.7, pp.1001-1010.

Hinton, M.J.; Kaddour, A.S.; Soden, P.D., 2002, "A comparison of the predictive capabilities of current failure theories for composite laminates, judge against experimental evidence", Composites Science and Technology, Vol.62, n. 12-13, pp.1725-1797.

Icardi, U.; Locatto, S.; Longo, A., 2007, "Assessment of recent theories for predicting failures of composite laminates", Applied Mechanics Reviews, Vol.60, n. 2, pp. 76-86.

Matthews, F.L and Rawlings, R.D., 1994, "Composite materials: engineering and science", Ed. Chapman & Hall, London.

Mendonça, P.T.R., 2005, "Materiais compostos e estruturas sanduíche: projeto e análise", Ed. Manole, Barueri, São Paulo.

Richardson, M.O.W. and Wisheart, M.J., 1996, "Review of low-velocity impact properties of composite materials", Composites, Part A, Vol. 27A, pp. 1123-1131.

Romariz, L.A., 2008, "Dano em placas laminadas devido ao impacto a baixas velocidades", Thesis (Master Degree), Universisdade de São Paulo, São Paulo, Brazil.

9. RESPONSIBILITY NOTICE

The authors are the only responsible for the printed material included in this paper.